

Electronic Supplementary Information (ESI)

Cationic Liposomes as Efficient Nanocarriers for the Drug Delivery of an Anticancer Cholesterol-based Ruthenium Complex

Giuseppe Vitiello,^{a,b} Alessandra Luchini,^{b,c} Gerardino D'Errico,^{b,c} Rita Santamaria,^d
Antonella Capuozzo,^d Carlo Irace,^d Daniela Montesarchio,^{c,*} Luigi Paduano^{b,c,*}

^a Department of Chemical, Materials and Production Engineering, University of Naples
“Federico II”, Piazzale Tecchio 80, 80125 Naples – Italy.

^b CSGI – Consorzio interuniversitario per lo sviluppo di Sistemi a Grande Interfase.

^c Department of Chemical Sciences, University of Naples “Federico II”, Via Cinthia 4,
80126 Naples, Italy.

^d Department of Pharmacy, University of Naples “Federico II”, Via D. Montesano 49,
80131 Naples, Italy.

*Corresponding Authors E-mail:

daniela.montesarchio@unina.it, luigi.paduano@unina.it

Phone: +390 81 674250. Fax: +390 81 674090.

Keywords: nanosystems; nucleolipid-based ruthenium (III) complex; cholesterol;
microstructural characterization; cellular uptake; biological activity.

Experimental

Dynamic Light Scattering (DLS)

DLS measurements were performed with a home-made instrument composed by a Photocor compact goniometer, a SMD 6000 Laser Quantum 50 mW light source operating at 5325 Å, a photomultiplier (PMT-120-OP/B) and a correlator (Flex02-01D) from *Correlator.com*.¹ The measurements were performed at (25.00 ± 0.05) °C with temperature controlled through the use of a thermostat bath. All the experiments were performed at the scattering angle of 90° (θ), the value of the scattering vector $q = 4\pi n / \lambda \sin(\theta/2)$ was calculated assuming the refractive index of the solution $n = 1.33$ for the water suspension and $n = 1.43$ for the cyclohexane suspension. The scattered intensity correlation function was analyzed using a regularization algorithm.² The measured diffusion coefficients was taken as the z-average diffusion coefficient of the obtained distributions.³

For spheres diffusing in a continuum medium at infinite dilution, the diffusion coefficient $\langle D \rangle \equiv \langle D \rangle_\infty$, and is dependent on the sphere radius R_H , called hydrodynamic radius, through the Stokes–Einstein equation:

$$R_H = \frac{kT}{6\pi\eta\langle D_\infty \rangle} \quad (1)$$

where k is the Boltzmann constant, T is the absolute temperature and η is the medium viscosity, assumed to be 0.89 cP for the water suspension and 1.02 cP for the cyclohexane suspension. For not spherical particles, R_H represents the radius of equivalent spherical aggregates. In this hypothesis, equation (1) can be reasonably used to estimate the average hydrodynamic radius of the aggregates.⁴

In the present case the R_H was estimated from at least three measurements of the diffusion coefficients of the aggregates for each analyzed samples.

Zeta Potential

Zeta potential measurements were performed with a Malvern Zetasizer Nano-ZS using the technique of laser Doppler velocimetry (LDV). In this technique, a voltage gradient is applied across a pair of electrodes at either end of the cell containing the particle

dispersion. Charged particles are attracted to the oppositely charged electrode and their velocity can be measured and expressed in unit field strength as an electrophoretic mobility, U_E . Before each experiment, fresh 100 ml aliquots were withdrawn from each sample, diluted 1:20 (v/v) with deionized water and left to equilibrate for 1–2 h at rest, at $T = 298$ K. The diluted samples were filled into disposable cells and the zeta potential (ζ) was determined at least three times for each type of particle systems. In order to check the Malvern device, a carboxy-modified polystyrene latex standard sample, with $\zeta = (68.0 \pm 6.8)$ mV at $T = 298$ K was used before each set of determinations as a control. The Malvern computer program was used to calculate the zeta potential ζ automatically from the measured U_E by using the Henry equation:

$$U_E = \frac{2\varepsilon\zeta}{3\eta} f(\kappa R) \quad (4)$$

where ε is the dielectric constant, η is the viscosity of media, R is the hydrodynamic radius of particle and κR the ratio of particle size to Debye length. For the conversion of mobility into $\zeta - f(\kappa R)$ potential the Smoluchowski factor $f(\kappa R) = 1.5$ was used, which in turn is valid under the limit $\kappa R \gg 1$. The instrument automatically optimizes the signal intensity within the range of 200–300 kcps, to keep the ratio of sample-to-reference count rates approximately constant. Effective voltage gradient was in the range 40–140 mV/mm.

Cryo-TEM

Cryo-TEM experiments were performed on a JEOL 200 kV JEM-FS2200 instrument with a field emission gun (FEG), with a magnification from 50x to 1500000x, a resolution of 0.2 nm in point and 0.1 nm in lattice. The microscope is equipped with a Tietz CCD camera with 2048×2048 pixels.

Small Angle Neutron Scattering (SANS)

SANS measurements were performed at 25 °C with the V4 instrument located at the Helmholtz Zentrum Berlin (Germany). A two-dimensional array detector at two different

wavelength (W)/collimation (C)/sample-to-detector (D) distance combinations ($W_{8\text{\AA}}C_{2m}D_{2m}$, and $W_{8\text{\AA}}C_{12m}D_{12m}$), measured neutrons scattered from the samples. These configurations allowed collecting data in a range of the scattering vector modulus $q = 4\pi/\lambda \sin(\theta/2)$ between 0.0025 \AA^{-1} and 0.209 \AA^{-1} , with θ indicating the scattering angle. The raw data were treated in order to subtract the background and the empty cell scattering. Furthermore detector efficiency was taken into account by measuring the scattering arising from a cell filled with H_2O , while for the radial average a cadmium beam-stop was positioned in the sample holder. Thus, the so obtained absolute scattering cross sections $d\Sigma/d\Omega$ data were plotted as function of q .

Generally, the dependence of $d\Sigma/d\Omega$ from the scattering vector can be expressed as follows:

$$\frac{d\Sigma}{d\Omega} = n_p P(q) S(q) + \left(\frac{d\Sigma}{d\Omega} \right)_{\text{incoh}} \quad (5)$$

Where n_p is the number of scattering objects, $P(q)$ and $S(q)$ are respectively the form factor and the structure factor, and the last term takes into account the incoherent scattering mostly due to the presence of hydrogen atoms within the sample.

The form factor is responsible for the shape, size distribution of the scattering particles, while a contribution of the structure factor can be considered when an interparticle correlation exists. The structural information contained in both the form and the structure factor can be extrapolated by choosing an appropriate model to fit the obtained experimental data. The experimental SANS profiles have been fitted by using SASview program, available on <http://www.sasview.org/>.

Neutron Reflectivity (NR)

NR allows to determine the structure and composition of layers at interfaces. Measurements were performed on the D17 reflectometer at the high flux reactor of the Institut Laue-Langevin (ILL, Grenoble, France) in time-of-flight mode using a spread of wavelengths between 2 and 20 \AA with two incoming angles of 0.8 and 3.2°. The specular reflection at the silicon/water interface, R , defined as the ratio between the reflected and the incoming intensities of a neutron beam, is measured as a function of the wave vector

transfer, q , perpendicular to the reflecting surface. $R(q)$ is related to the scattering length density across the interface, $\rho(z)$, which depends on the composition of the adsorbed species.

The scattering lengths of the constituent fragments of any species adsorbed at the surface are the fundamental quantities from which the interfacial properties and microstructural information on the lipid bilayer are derived. Measurement of a sample in different solvent contrasts greatly enhances the sensitivity of the technique.⁵⁻⁷ Samples were measured using H₂O, SMW (silicon-matched water) and D₂O as solvent contrasts. SMW ($\rho = 2.07 \times 10^{-6} \text{ \AA}^{-2}$) is a mixture of 38 vol % D₂O ($\rho = 6.35 \times 10^{-6} \text{ \AA}^{-2}$) and 62 vol % H₂O ($\rho = 0.56 \times 10^{-6} \text{ \AA}^{-2}$) with the same refraction index for neutrons as a bulk silicon.

NR profiles were analysed by box model fitting, starting with simulations from the AFIT program.⁸ The supported membrane is modelled as a series of boxes corresponding to the different bilayer regions. The program allows the simultaneous analysis of reflectivity profiles from the same sample in different water contrasts, characterizing each box by its thickness, scattering length density (ρ), solvent volume fraction, and interfacial roughness. These initial model fits were then used as templates for simultaneous fitting of the experimental data using the MOTOFIT program.⁹ All the parameters were varied until the optimum fit to the data was found. Although more than one model could be found for a given experimental curve, the number of possible models was greatly reduced on the basis of prior knowledge of the system, which allows defining upper and lower limits of the parameters to be optimized, of the elimination of the physically meaningless parameters, and most importantly of the use of different isotopic contrasts.⁹ The bare silicon substrate was characterized first in terms of thickness and roughness of the native oxide layer. The set of NR profiles were calculated for a uniform single layer model (the silicon oxide layer) of thickness $8 \pm 1 \text{ \AA}$, roughness $3 \pm 1 \text{ \AA}$, and a scattering length density of $3.41 \times 10^{-6} \text{ \AA}^{-2}$, corresponding to 100% SiO₂.

Electronic Paramagnetic Resonance (EPR)

EPR spectra were recorded on a 9 GHz BrukerElexys E-500 spectrometer (Bruker, Rheinstetten, Germany). Capillaries containing the samples were placed in a standard 4 mm quartz sample tube containing light silicone oil for thermal stability. The temperature

of the sample was regulated at 25 °C and maintained constant during the measurement by blowing thermostated nitrogen gas through a quartz Dewar. The instrumental settings were as follows: sweep width, 120 G; resolution, 1024 points; modulation frequency, 100 kHz; modulation amplitude, 1.0 G; time constant, 20.5 ms, incident power, 5.0 mW. Several scans, typically 16, were accumulated to improve the signal-to-noise ratio.

A quantitative analysis of *n*-PCSL spectra for all the lipid samples was realized determining the acyl chain order parameters, S , and the isotropic hyperfine coupling constants for the spin-labels in the membrane, a'_N , as described in the literature.^{10,11} S is a measure of the local orientational ordering of the labelled molecule with respect to the normal to the bilayer surface, while a'_N is an index of the micropolarity experienced by the nitroxide. Both S and a'_N decrease progressively with increasing n , as the spin-label position is stepped down the chain toward the center of the membrane.

Cell cultures and *in vitro* bioscreenings

Human WiDr epithelial colorectal adenocarcinoma cells, HeLa cervical adenocarcinoma cells, MCF-7 breast adenocarcinoma cells, HaCaT keratinocytes, and rat L6 skeletal muscle cells were all purchased from ATCC (American Type Culture Collection, Manassas, Virginia, USA). MCF-7 and WiDr cells were grown in RPMI 1640 medium (Invitrogen, Paisley, UK), whereas HeLa, HaCaT and L6 cells were grown in DMEM (Invitrogen, Paisley, UK). Media were supplemented with 10% fetal bovine serum (FBS, Cambrex, Verviers, Belgium), L-glutamine (2 mM, Sigma, Milan, Italy), penicillin (100 units/ml, Sigma) and streptomycin (100 µg/ml, Sigma), according to ATCC recommendations. The cells were cultured in a humidified 5% carbon dioxide atmosphere at 37 °C.

The anticancer activity of ruthenium-containing nucleolipidic nanoparticles and AziRu was investigated through the estimation of a “cell survival index”, arising from the combination of cell viability evaluation with cell counting. Cells were inoculated in a standard sterile plastic 96-microwell culture plates at a density of 10^4 cells/well. Cells were allowed to grow for 24 h, then the medium was replaced with fresh medium and cells were treated for further 48 h with a range of concentrations (10→1000 µM) of

AziRu and ToThyCholRu complex lodged in POPC or DOTAP liposomes (ToThyCholRu/POPC and ToThyCholRu/DOTAP, respectively). Using the same experimental procedure, cell cultures were also incubated with Ruthenium-free ToThyChol/POPC and ToThyChol/DOTAP liposomes as negative controls, as well as with cisplatin (cDDP) - a positive control for cytotoxic effects. Cell viability was evaluated with the MTT assay procedure, which measures the level of mitochondrial dehydrogenase activity using the yellow 3-(4,5-dimethyl-2-thiazolyl)-2,5-diphenyl-2H-tetrazolium bromide (MTT, Sigma) as substrate. The assay is based on the redox ability of living mitochondria to convert dissolved MTT into insoluble purple formazan. Briefly, after the treatments, the medium was removed and the cells were incubated with 20 μ l/well of a MTT solution (5 mg/mL) for 1 h in a humidified 5% CO₂ incubator at 37 °C. The incubation was stopped by removing the MTT solution and by adding 100 μ l/well of DMSO to solubilize the formazan. Finally, the absorbance was monitored at 530 nm by using a multiwell plate-reader in a Perkin-Elmer LS 55 Luminescence Spectrometer (Perkin-Elmer Ltd, Beaconsfield, UK).¹²

Cell number was determined by TC10 automated cell counter (Bio-Rad, Milan, Italy), providing an accurate and reproducible total count of cells and a live/dead ratio in one step by a specific dye (trypan blue) exclusion assay. Following the same principle used in hemocytometers, Bio-Rad's TC10 automated cell counter uses disposable slides, TC10 trypan blue dye (filter-sterilized 0.4% trypan blue dye w/v in 0.81% sodium chloride and 0.06% potassium phosphate dibasic solution) and a CCD camera to count cells based on the analyses of captured images. Once the loaded slide is inserted into the slide port, the TC10 automatically focuses on the cells, detects the presence of trypan blue dye and provides the count. When cells are damaged or dead, trypan blue can enter the cell allowing dead cells to be counted. Operationally, after bioscreen incubations in standard 96-microwell culture plates, the medium was removed and the cells were collected. Ten microliters of cell suspension, mixed first with 0.4% trypan blue solution at 1:1 ratio, were directly loaded into the chambers of disposable slides. The results are displayed as total cell count (number of cells per ml). If trypan blue is detected, the instrument also accounts for the dilution and shows live cell count and percent viability. Total counts and

live/dead ratio from random samples for each cell line were subjected to comparisons with manual hemocytometers in control experiments.

The calculation of the concentration required to inhibit the net increase in the cell number and viability by 50% (IC₅₀) is based on plots of data ($n = 6$ for each experiment) and repeated five times (total $n = 30$). IC₅₀ values were obtained by means of a dose response curve by nonlinear regression using a curve fitting program, GraphPad Prism 5.0, and are expressed as mean \pm SEM ($n = 30$) of five independent experiments.

Fluorescence microscopy and cellular uptake of liposomes

Non autofluorescent poly-D-lysine coated sterile glass coverslips (neuVITRO, El Monte, CA, USA) were placed in standard sterile plastic 24-well plates and human MCF-7 cells and WiDr adenocarcinoma cells were seeded at a density of 4×10^4 /well. Following a growth period of 24 h at 37 °C in RPMI 1640 medium containing 10% FBS, the cells were incubated for additional times (30 min, 1, 3 and 6 h) with 100 μ M of ToThyCholRu/DOTAP liposomes containing a fluorescent rhodamine B derivative,¹³ as reported in sample preparation. After incubations, unassociated liposomes were removed by PBS washing (three times) and the cells were then fixed at room temperature in 4% paraformaldehyde for 20 minutes. After three washings with PBS, the cells were treated with diaminophenylindole (DAPI) (Sigma) to stain the nuclei. The coverslip from each well was mounted onto a glass microslide with 80% fluorescence-free glycerol mounting medium. Finally, the interaction of liposomes with MCF-7 and WiDr cells and their cellular uptake was monitored using a fluorescent microscope (Leica Microsystems GmbH, Wetzlar, Germany) to visualize DAPI (360/460 nm), and rhodamine B (560/583 nm) fluorophores. Images at 100 \times total magnification (10 \times objective and a 10 \times eyepiece) were taken using an AxioCamHRc video-camera (Zeiss) connected to an Axioplan fluorescence microscope (Zeiss) using the AxioVision 3.1 software. Merged images (Merged) are obtained by overlapping DAPI and rhodamine B fluorophores emission emerging from the same cell monolayers.

Light Microscopy

MCF-7, WiDr and HeLa cell lines were grown on standard sterile plastic 60 mm culture dishes by plating 5×10^5 cells. After reaching the subconfluence, cells were incubated for 48 h with 50 μ M concentration of ToThyCholRu/DOTAP liposomes under the same *in vitro* experimental conditions described above. Finally, cells were observed by a contrast-phase light microscope (Labovert microscope, Leizt). Microphotographs at a $200 \times$ total magnification ($20 \times$ objective and $10 \times$ eyepiece) were taken with a standard VCR camera (Nikon).

DNA fragmentation assay

MCF-7, WiDr and HeLa cell lines were grown on standard sterile plastic 60 mm culture dishes by plating 5×10^5 cells. After 24 h of growth the cells were treated for 48 h with IC_{50} doses of ToThyCholRu/DOTAP liposomes under the same *in vitro* experimental conditions described for bioscreens, as well as with IC_{50} doses of cisplatin (cDDP) - a positive control for *in vitro* apoptosis.¹⁴ Then, the cells were collected and the pellets were suspended in lysis buffer (50 mM Tris-HCl, pH 8.0, 5 mM EDTA, 100 mM NaCl, 1% SDS, 0.5 mg/mL Proteinase K) and incubated at 50°C. After 1 h incubation, 10 mg/mL RNase was added to the lysates and incubated for 1 h at 50°C. DNA was precipitated with NaOAc pH 5.2 and ice cold 100% EtOH and centrifuged at $14000 \times g$ for 10 min. Pellets were dissolved in TE buffer (10 mM Tris-HCl, pH 8.0, 1 mM EDTA). A 20 μ L aliquot of each DNA sample was analyzed on a 1.5 % agarose gel stained with ethidium bromide and visualized under UV light.

Statistical Analysis

All data were presented as mean \pm SEM. The statistical analysis was performed using Graph-Pad Prism (Graph-Pad software Inc., San Diego, CA) and ANOVA test for multiple comparisons was performed followed by Bonferroni's test.

Table ESI1 - Molecular properties of pure DOTAP and ToThyCholRu complex-containing DOTAP aggregate. Data for molecular volumes of complex headgroups have been evaluated through the Volume keyword available in Gaussian 09 package. The molecular volume of the hydrophobic chains has been evaluated according to Tanford, while the molecular volume of cholesterol is taken from literature data.⁷ Finally, data for the oligoethoxyethylene glycol (OEG) lateral chains have been acquired elsewhere.¹³

	DOTAP	ToThyCholRu
V_{chains}	550 \AA^3	361 \AA^3
$10^6 \times \rho_{\text{chains}}$	-0.46 \AA^{-2}	-0.22 \AA^{-2}
$V_{\text{headgroup}}$	220 \AA^3	440 \AA^3
$10^6 \times \rho_{\text{headgroup}}$	0.76 \AA^{-2}	1.04 \AA^{-2}
V_{OEG}		240 \AA^3
$10^6 \times \rho_{\text{OEG}}$		0.65 \AA^{-2}

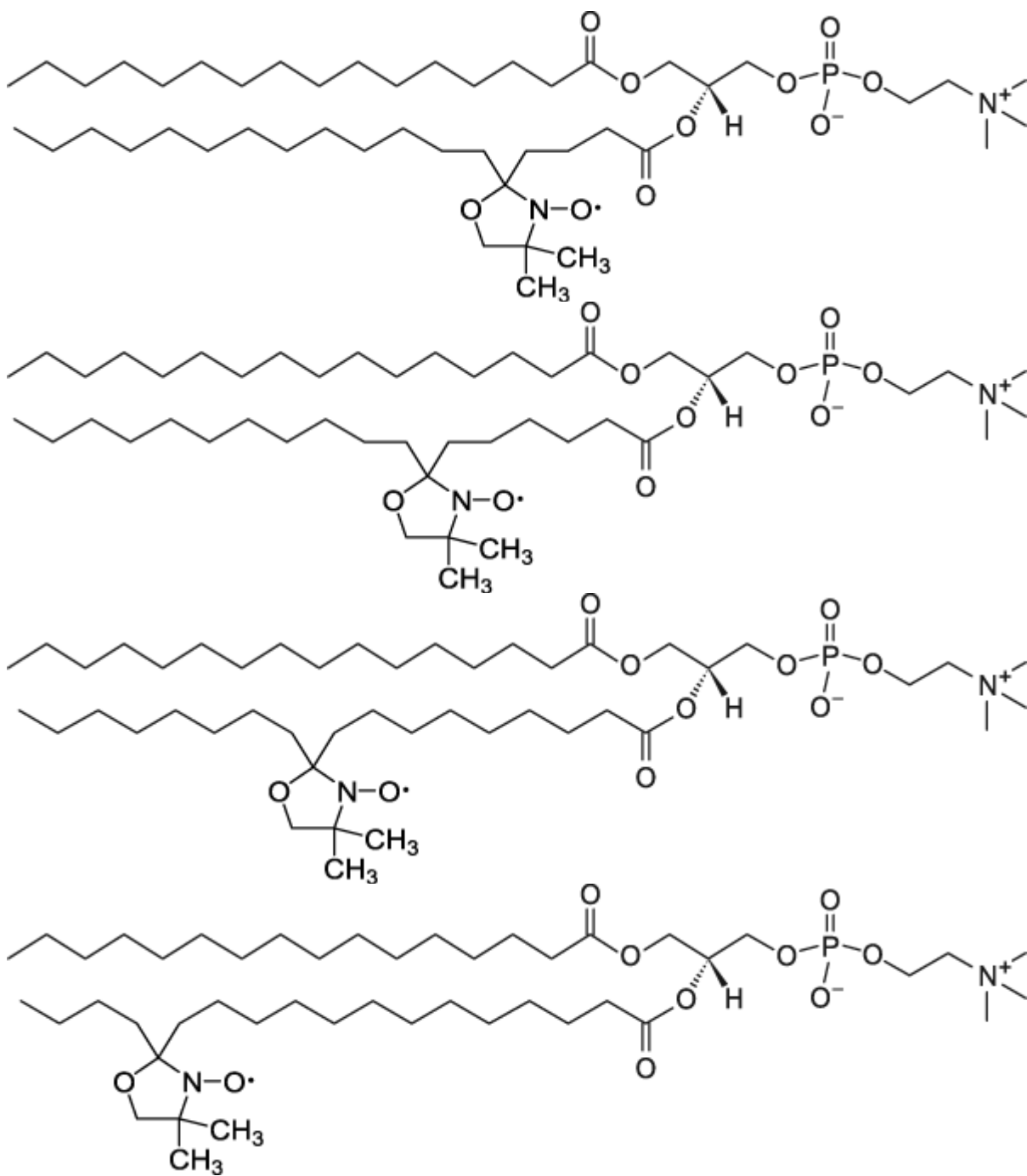


Figure ESI1 – Molecular structures of 5-PCSL, 7-PCSL, 10-PCSL and 14-PCSL spin-labels.

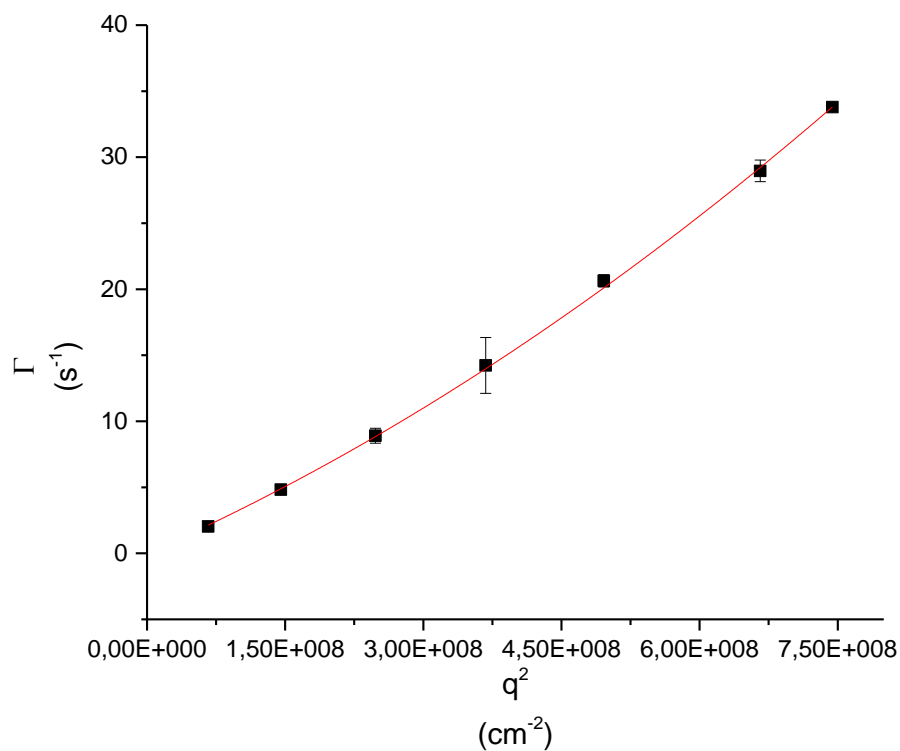


Figure ESI2 - Experimental values of Γ as function of q^2 for ToThyCholRu/DOTAP 30/70 liposomes. The experimental data were interpolated using the following equation: $\Gamma = B1 \cdot (q^2) + B2 \cdot (q^2)^2$, with the following fitting parameters, $B1 = (3.07 \pm 0.07)10^{-8}$, $B2 = (1.97 \pm 0.09) 10^{-17}$.

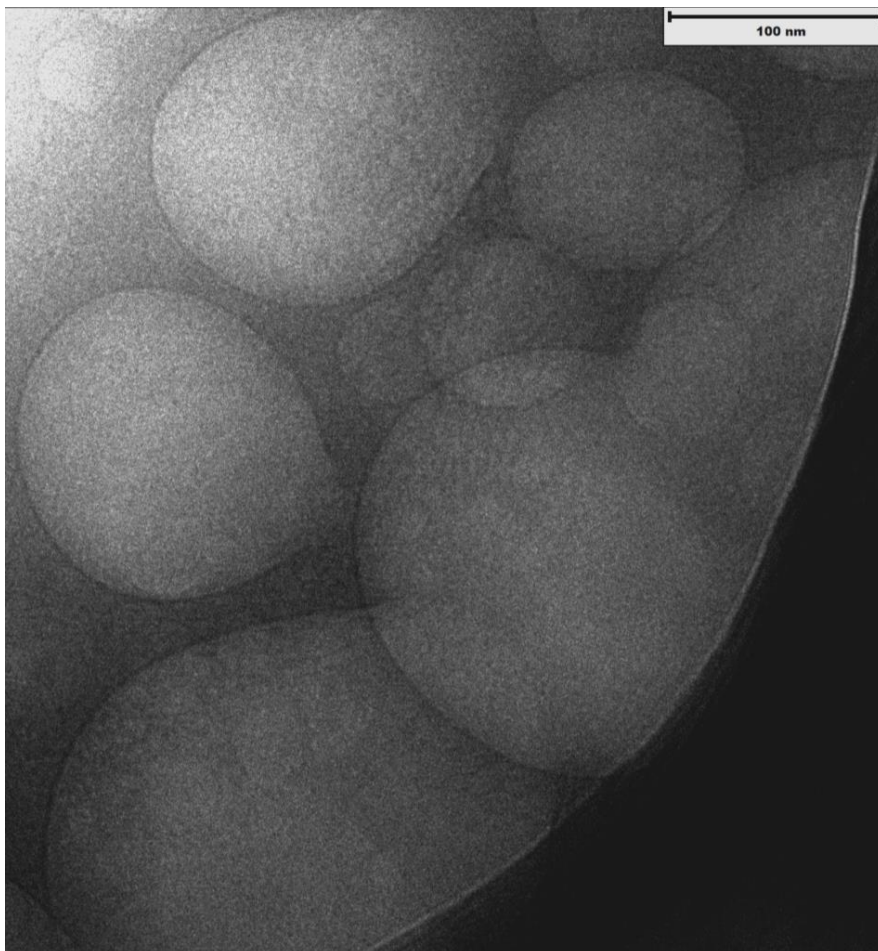


Figure ESI3 – A cryo-TEM image of ToThyCholRu /DOTAP liposomes.

References

1. G. Mangiapia, G. D'Errico, L. Simeone, C. Irace, A. Radulescu, A. Di Pascale, A. Colonna, D. Montesarchio and L. Paduano, *Biomaterials*, 2012, 33(14), 3770-3782.
2. A. Lomakin, D. B. Teplow and G. B. Benedek in *Methods in Molecular Biology Amyloid Proteins*, vol. 299: *Methods and Protocols*, E. M. Sigurdsson, Ed. Humana Press, Totowa, NJ, 2005, 153–174.
3. H. Zhang and O. Annunziata, *J. Phys. Chem. B* 2008, 112, 3633–3643.
4. L. Paduano, R. Sartorio, G. D'Errico and V. Vitagliano, *Faraday Trans.* 1998, 94(17), 2571-2576.
5. G. Fragneto, J. R. Lu, D. C. McDermott, R. K. Thomas, A. R. Rennie, P. D. Gallagher and S. K. Satija, *Langmuir*, 1996, 12, 477-486.
6. A. Merlino, G. Vitiello, M. Grimaldi, F. Sica, E. Busi, R. Basosi, A. M. D'Ursi, G. Fragneto, L. Paduano and G. D'Errico, *J Phys Chem B*, 2012, 116, 401-412.
7. G. Vitiello, G. Fragneto, A. A. Petruk, A. Falanga, S. Galdiero, A. M. D'Ursi, A. Merlino and G. D'Errico, *Soft Matter*, 2013, 9, 6442-6456.
8. P. N. Thirtle, Z. X. Li, R. K. Thomas, A. R. Rennie, S. K. Satija and L. P. Sung, *Langmuir*, 1997, 13, 5451-5458.
9. A. Nelson, *J Appl Crystallogr*, 2006, 39, 273-276.
10. S. Galdiero, A. Falanga, G. Vitiello, M. Vitiello, C. Pedone, G. D'Errico and M. Galdiero, *BBA-Biomembranes*, 2010, 1798, 579-591.
11. G. Vitiello, A. Falanga, M. Galdiero, D. Marsh, S. Galdiero and G. D'Errico, *BBA-Biomembranes*, 2011, 1808, 2517-2526.
12. F. Fiorito, C. Irace, A. Di Pascale, A. Colonna, G. Iovane, U. Pagnini, R. Santamaria and L. De Martino, *Plos One*, 2013, 8, e58845.
13. G. Mangiapia, G. Vitiello, C. Irace, R. Santamaria, A. Colonna, R. Angelico, A. Radulescu, G. D'Errico, D. Montesarchio and L. Paduano, *Biomacromolecules*, 2013, 14, 2549-2560.
14. M. Okamura, K. Hashimoto, J. Shimada and H. Sakagami, *Anticancer Research*, 2004, 24, 655-662.